Hindawi
Journal of Nanomaterials
Volume 2019, Article ID 2341268, 9 pages
https://doi.org/10.1155/2019/2341268

Research Article

Stable Electrochemical Measurements of Platinum Screen-Printed Electrodes Modified with Vertical ZnO Nanorods for Bacterial Detection

Thi Hong Phuoc Nguyen,[1] Matteo Tonezzer,[1] Thi Thanh Le Dang,[1] Quang Khue Vu,[2] Quang Huy Tran,[3] Duc Hoa Nguyen,[1] and Van Hieu Nguyen[4,5]

[1]*International Training Institute of Materials Science (ITIMS), Hanoi University of Science and Technology (HUST), 1-Dai Co Viet Road, Hanoi, Vietnam*
[2]*AIST, Hanoi University of Science and Technology (HUST), 1-Dai Co Viet Road, Hanoi, Vietnam*
[3]*National Institute of Hygiene and Epidemiology, 1 Yersin Street, Hanoi, Vietnam*
[4]*Faculty of Electrical and Electronic Engineering, Phenikaa Institute for Advanced Study (PIAS), Phenikaa University, Yen Nghia, Ha Dong District, Hanoi, Vietnam*
[5]*Phenikaa Research and Technology Institute (PRATI), A&A Green Phoenix Group, 167 Hoang Ngan, Hanoi, Vietnam*

Correspondence should be addressed to Thi Thanh Le Dang; thanhle@itims.edu.vn and Quang Huy Tran; tqh@nihe.org.vn

Received 25 February 2019; Revised 24 May 2019; Accepted 19 June 2019; Published 1 August 2019

Guest Editor: Zhen Yu

The study is aimed at investigating the stability of electrochemical and biosensing properties of ZnO nanorod-based platinum screen-printed electrodes (SPEs) applied for detection of bacterial pathogens. The platinum SPEs were designed and patterned according to standard photolithography and lift-off process on a silicon wafer. ZnO nanorods (NRs) were grown on the platinum working electrode by the hydrothermal method, whereas *Salmonella* polyclonal antibodies were selected and immobilized onto ZnO NR surface via a crosslinking process. Morphological and structural characteristics of ZnO NRs were investigated by scanning electron microscopy (SEM), transmission electron microscopy (TEM), and X-ray diffraction (XRD). The results showed that the ZnO NRs were grown vertically on platinum electrodes with a diameter around 20-200 nm and a length of 5-7 μm. These modified electrodes were applied for detection of *Salmonella enteritidis* at a concentration of 10^3 cfu/mL by electrochemical measurements including cyclic voltammetry (CV) and electrochemical impedance spectroscopy (EIS). The ZnO NR-modified platinum electrodes could detect *Salmonella* bacteria well with stable measurements, and the signal to noise ratio was much higher than that of 3 : 1. This study indicated that ZnO NR-modified platinum SPEs could be potential for the development of biochips for electrochemical detection of bacterial pathogens.

1. Introduction

Electrochemical biosensors have recently attracted much attention because of their potential applications in food safety, environmental pollution monitoring, pharmaceutical chemistry, and clinical diagnostics [1–3]. The electrochemical biosensors have many advantages such as easy operation, low cost, high sensitivity, a simple instrument, and suitability for portable devices [4]. However, these platforms require a stable surface over time for specific applications; it will help the system to improve the electron transfer between electrolytic solution and electrode and minimize the loss of biological molecules during the electrochemical process. Carbon screen-printed electrodes (SPEs) are normally used for detection of biological molecules, but they seem more preferable for enzyme-based biosensors with enzymatic redox reactions than for deoxyribonucleic acid (DNA) or immuno-based biosensors [5, 6]. Platinum SPEs are also developed for various purposes. Thanks to their electronic properties and a narrow area of the working electrode, the

electron transfer would occur easily [7]. However, it also leads to a limitation of the contact space with targets and the existence of biological molecules on the surface of electrodes during the electrochemical process. Some advanced nanomaterials have been proposed to solve the problem and also enhance the sensor performance [8, 9].

Nanostructured metal oxides are quite attractive for biosensor applications thanks to their biocompatibility and advanced physical and chemical properties [10]. The advantages of nanostructured metal oxides involve the surface-charged depletion and efficient charge-transfer catalytic properties which enable them to become a useful solid support for antibody immobilization in biosensors [11]. Among others, zinc oxide (ZnO), a nontoxicity *n*-type semiconductor with wide band gap (3.37 eV), high chemical stability, good electrical properties, high isoelectric point (pH 9–9.5), and high electron transfer capability, is one of the most interesting metal oxides used for biosensors [12–14]. Recently, ZnO nanorods (NRs) have also revealed advantages in biosensors, such as good reproducibility, high sensitivity, and cost-effective fabrication techniques as well as portability [15]. There are several ways reported to deposit ZnO nanorods on substrates such as dielectrophoresis [16], focused-ion-beam [17], or chemical vapour deposition [18]. This material can be easily synthesized in the nanorod shape by the fast, low temperature, and inexpensive hydrothermal route [19, 20]. Besides, the hydrothermal route can be performed at low temperature to grow ZnO NRs on-chip [21]. However, most reports of ZnO NR electrochemical-based biosensor rely on the traditional three-electrode system involving separated platinum wire counter electrode, ZnO NR working electrode, and a reference electrode. The use of traditionally separated electrodes suffers from a complex configuration of the sensor measurement system and consumes a large number of bioreceptors [22].

In the strategy of developing a new type of electrochemical biochips for quick and accurate detection of bacterial pathogens, ZnO NR-modified platinum SPEs have been developed, and *Salmonella* bacteria is selected for testing the stability of electrochemical and biosensing properties of single-modified electrodes. Recently, *Salmonella* species infection has posed a serious threat to public health, especially in developing countries, where people use poultry meats and food-producing animals without control measures [14, 19, 20]. In Vietnam, it is reported that *Salmonella*, a bacterial pathogen, is present in most animal-origin foods including poultry, ovines, porcines, fish, and seafood and their food products [23]. Furthermore, some *Salmonella*-contaminated fruits and fresh vegetables are also reported to be associated with the *Salmonellosis* [24–26]. However, detecting *Salmonella* is time-consuming and labour-intensive, because the conventional methods require isolation, preenrichment, or genome amplification [27]. Development of a rapid and reliable method, especially biochip for electrochemical detection of the presence of these pathogens at a low concentration, is also a very important mission for point-of-care applications.

In this study, we designed and fabricated the ZnO NR-modified platinum (Pt) compact electrodes by integration of counter, working, and pseudoreference electrodes on a chip. In the design, Pt is used as both counter and pseudoreference electrodes, whereas vertically grown ZnO NRs act as working electrode. We also investigated the stability of the electrochemical signal of the ZnO NR-modified Pt SPEs before and after antibody immobilization and the detection of *Salmonella* bacteria. The success of the study will help fabricate multimodified sensors on a biochip for further direct detection of bacterial pathogens.

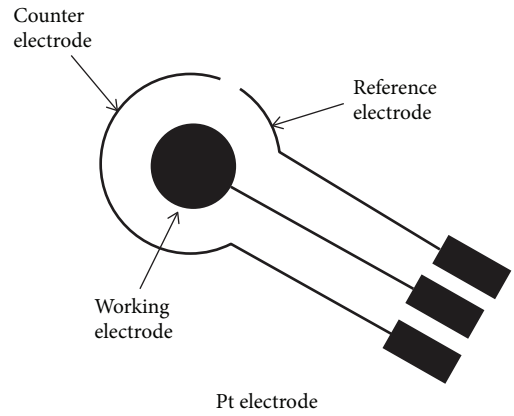

Scheme 1: Design of a platinum based on the SPE.

2. Experimental

2.1. Reagents and Materials. Rabbit anti-*Salmonella* IgG polyclonal antibody, *Salmonella enteritidis* (ATCC 13076), and *Escherichia coli* (ATCC 25923) (10^6 cfu/mL, each) were provided by the Department of Bacteriology, National Institute of Hygiene and Epidemiology, Vietnam. Phosphate-buffered saline (PBS) buffer, bovine serum albumin (BSA), (3-mercaptopropyl)trimethoxysilane (MTS), N-(γ-maleimidobutyryloxy)-sulphosuccinimide ester (GMBS), zinc nitrate hexahydrate ($Zn(NO_3)_2{\cdot}6H_2O$), and hexamethylenetetramine (HMTA) were from Sigma-Aldrich. All chemicals were of analytical grade and used without any further purification. Deionized (DI) water (>18 MΩ) obtained from the Milli-Q purifying system was used in this study.

2.2. Fabrication of ZnO Nanorod Matrix/Electrode. The platinum SPEs were designed and patterned according to standard photolithography and lift-off process on a 4-inch silicon wafer. The design of platinum SPE is shown in Scheme 1, which includes Cr/Pt counter, working, and pseudoreference electrodes. The double layer of Cr/Pt (20/150 nm thickness) was deposited on a Si wafer covered with 300 nm of SiO_2 using a sputtering system. The thin Cr layer promotes adhesion of the Pt layer. The circular working electrode has a diameter of 4 mm, and the area covered by the electrodes is 12.56 mm^2, as in our previous publication [28]. A 20 nm of Zn seed layer was deposited by direct current (DC) sputtering on the Pt layer of the circular working electrode in order to grow the ZnO NRs thanks to our experience published previously [29, 30] (Figure 1(a)).

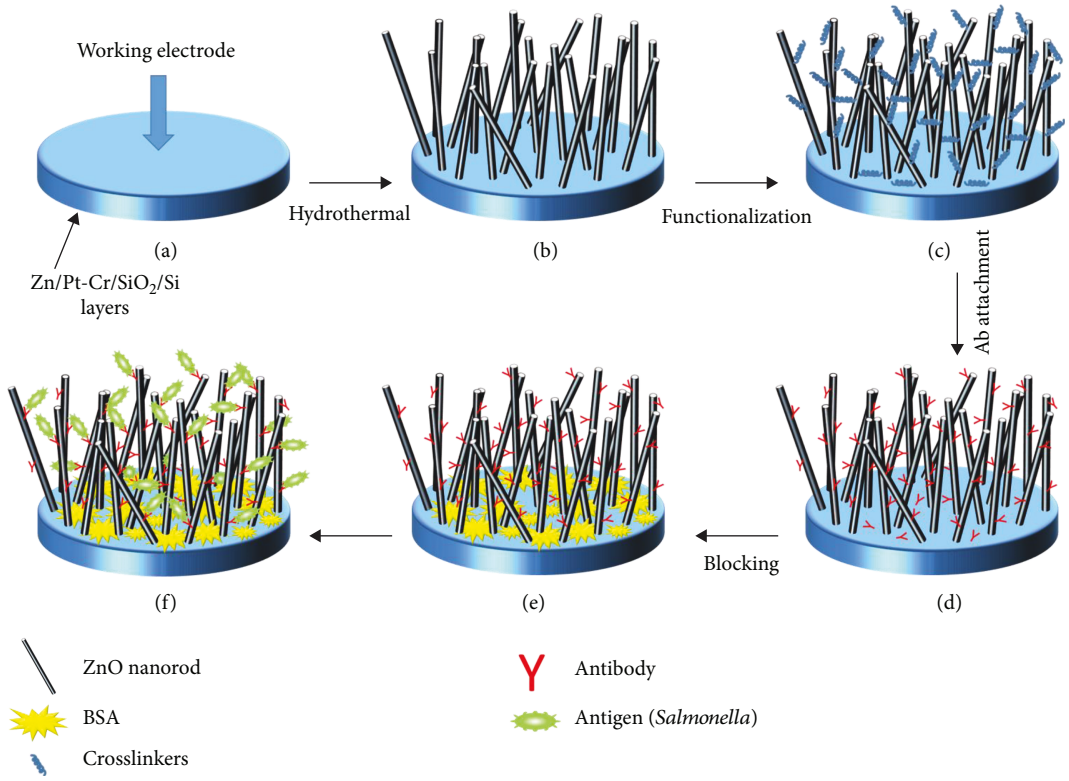

Figure 1: The schematic outline of the fabrication of on-chip electrochemical electrodes based on ZnO NRs: (a) deposition of Zn/Pt electrode on the silicon substrate, (b) growth of ZnO NRs, (c) functionalization of ZnO NRs with silane and GMBS, (d) antibody immobilization, (e) blocking the unspecific ZnO NR sites by using BSA, and (f) binding of bacterial antigens on the surface of the working electrode via specific antibodies immobilized in advance.

Figure 1 describes the whole preparation of ZnO NR-modified Pt SPEs for electrochemical detection of bacterial pathogens. After the growth of ZnO NRs on the Pt working electrode, they were functionalized by crosslinkers to provide active sites for antibody immobilization. Then, nonspecific binding sites were blocked by BSA. Finally, bacterial pathogens were added on the working electrode for testing by using electrochemical measurements.

ZnO NRs were vertically grown by a hydrothermal method, as reported elsewhere [15]. Briefly, an aqueous solution of 0.02 M zinc nitrate hexahydrate ($Zn(NO_3)_2{\cdot}6H_2O$) and 0.02 M hexamethylenetetramine (HMTA) was prepared in deionized water (Mili-Q). After vigorously stirring (700 rpm) the mixture solution for 2 h at 25°C, the microelectrodes were loaded upside down in the solution, and then, the temperature was increased to 80°C. After 24 h of deposition, the ZnO-coated electrodes were washed in deionized water and dried with an N_2 jet (Figure 1(b)).

2.3. Functionalization. Rabbit anti-*Salmonella* IgG polyclonal antibodies were immobilized onto the surface of ZnO NRs by crosslinking with N-[gamma-maleimidobutyryloxy] succinimide (GMBS). This heterobifunctional crosslinker contains N-hydroxysuccinimide (NHS) ester and maleimide groups that allow covalent conjugation with amino acid side chains presenting amine and sulfhydryl groups. The immobilization process includes silanization and crosslinking, as shown in Figure 2.

In the silanization step (Figure 2(a)), the ZnO NR electrode was submerged in a 2% solution of (3-mercaptopropyl)trimethoxysilane (MTS)/ethanol for 1 h. To remove the unbounded MTS, the silanized ZnO NRs were then washed in the solvent and finally dried with an N_2 jet. Attachment of the MTS molecules to the ZnO NR surface was reported to be predominantly through the silane groups with the sulfhydryl groups molecularly oriented away from the surface [31]. As metal oxides have hydroxyl groups on their surfaces, the interaction with silanes (MTS) leads to the formation of covalent -O-Si- groups between the surface and the crosslinking agent, as shown in Figure 2(a). MTS is a feasible option for functionalizing ZnO-based biosensors because it is a commercially available chemical and provides high antibody surface coverage with good uniformity [32, 33]. Therefore, this stage makes sulfhydryl (-SH) groups available at the surface of the ZnO NRs for further linking to the maleimide region of the secondary crosslinker GMBS in an organic solvent [34]. In the crosslinking step (Figure 2(b)), 5 μL of the GMBS was spread over the silanized ZnO NRs and left to incubate for 1 h at room temperature. During this process, the maleimide region of the conjugate GMBS binds to the sulphydryl groups present on the silanized surface of the ZnO. Covalent conjugation is possible by the attachment of the NHS ester groups of the GMBS to the amine groups of the antibody (Figure 2(c)). At the end, the prepared sensors were washed in PBS solution and dried with N_2 jet (Figure 1(c)).

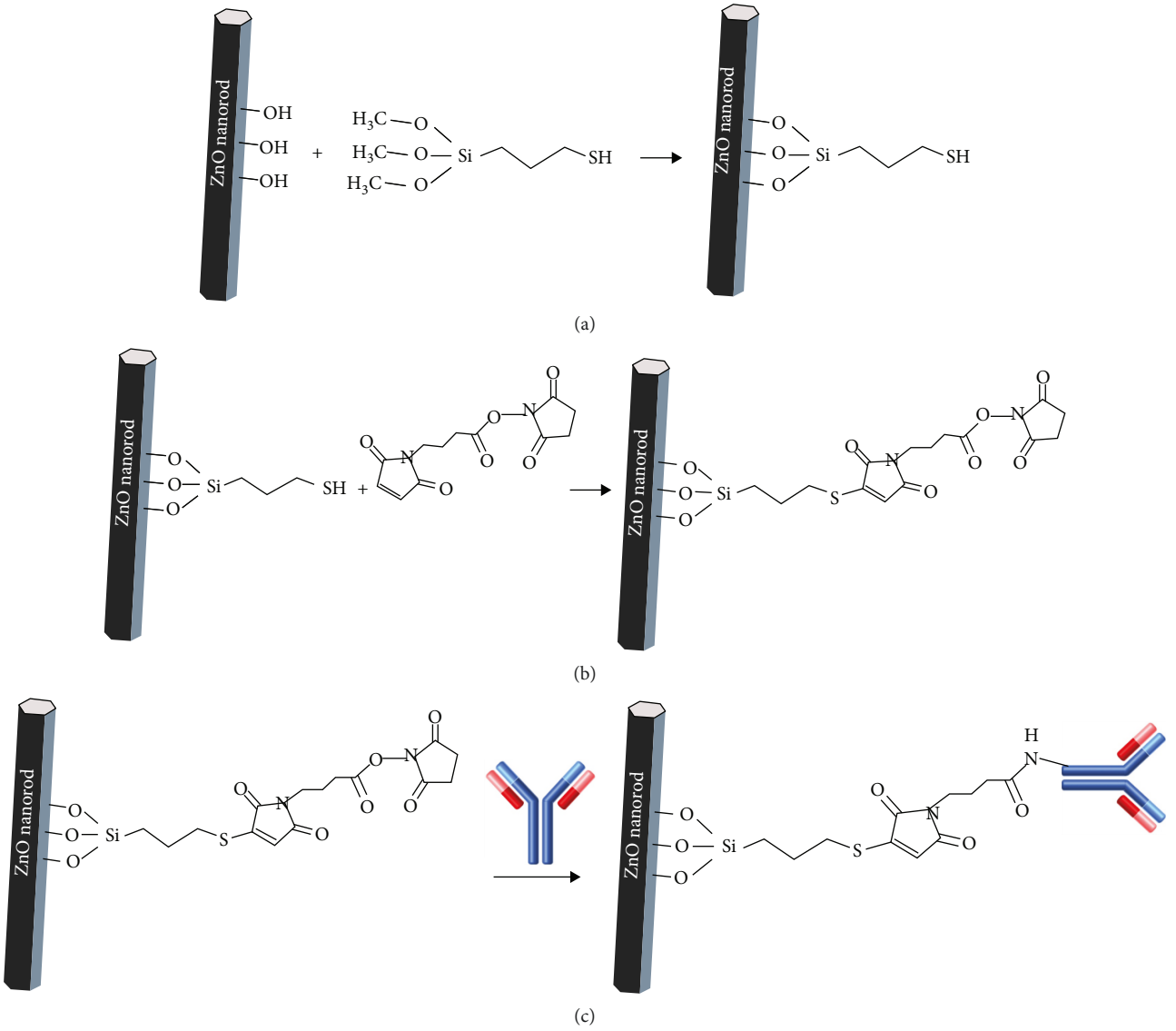

Figure 2: Antibody immobilization on ZnO NRs via GMBS crosslinker: (a) silanization the surface of the ZnO NRs, (b) conjugation of the crosslinker GMBS to the silanized ZnO NRs, and (c) conjugation of the antibody with the crosslinking moiety.

2.4. Preparation of the Electrochemical Biosensor Based on ZnO NR-Modified Pt SPEs. All reagents and vials were stored at 4°C during preparation and were left at room temperature just before analysis. In order to immobilize the antibody on the ZnO NR matrix electrode, the antibody solution was prepared by dilution in a 0.01 M phosphate-buffered saline (PBS) solution (pH 7.4). In order to investigate electrochemical and biosensing properties of ZnO NR-modified Pt SPEs, a fixed concentration of 2 μg/mL of anti-*Salmonella* IgG polyclonal antibody has been selected for capturing the working electrode [32, 33]. The antibody was dropped onto the functionalized ZnO NR matrix working electrodes and incubated for 60 min at room temperature to maximize the binding of antibody to ZnO NRs (Figure 1(d)). Following the antibody immobilization, a 5 μL 0.2% BSA/PBS (0.01 M, pH 7.4) was dropped onto the surface of the working electrodes in order to block the blank space (Figure 1(e)) and also cover nonspecific binding sites, then left them in incubation for further 60 min [4]. The electrodes were washed twice in PBS to remove loosely bound antibodies. Afterwards, 5 μL of *Salmonella* bacteria diluted in PBS (0.01 M, pH 7.4) at a concentration of 10^3 cfu/mL was dropped onto the modified working electrode and incubated for 30 min at room temperature, then washed in PBS (0.01 M, pH 7.4) to remove unbound components (Figure 1(f)). Similarly, positive and negative controls were performed with *E. coli* at a concentration of 10^6 cfu/mL and 0.2% BSA/PBS (0.01 M, pH 7.4), respectively. After drying the electrodes under gentle N_2 flow, they were analyzed by electrochemical measurements. Expectedly, during incubation, antigens of *Salmonella* would bind specifically to antibodies on the surface of electrodes, forming an insulating immune complex between *Salmonella* antibody and antigens, which inhibits electron transfer from the electrolytic solution to the electrode and

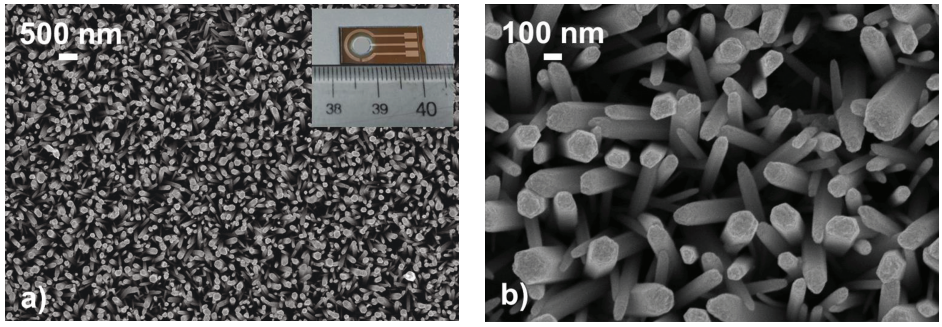

(a) (b)

Figure 3: SEM images of ZnO NRs on the Pt working electrode at different magnifications: (a) low magnification; (b) high magnification. Inset: a picture of a sensor chip.

further changes in the electron transfer resistance. All electrochemical measurements and testing were repeated with five sensors which have similar electrochemical properties.

2.5. Characterization and Electrochemical Measurements. Morphology and structure of ZnO NRs were studied by field effect scanning electron microscopy (FESEM, S4800; Hitachi) and high-resolution transmission electron microscopy (HRTEM, JEM 2100, JEOL). The crystalline structure was analyzed by XRD (Rigaku Smart Lab®System) with Cu Kα radiation operating at 40 kV and 40 mA. Electrochemical measurements were performed by a PalmSens3 (Netherlands). Cyclic voltammetry (CV) and electrochemical impedance spectra (EIS) were recorded in a 5 mM $K_3[Fe(CN)_6]/K_4[Fe(CN)_6]$ solution. For CV, the potential was cycled between -0.6 V and +0.6 V at a scan rate of 100 mV/s. The EIS measurements were performed in the frequency range from 50 mHz to 20 kHz around the open-circuit potential using an alternating-current probe with amplitude of 10 mV.

3. Results and Discussion

3.1. Characterization of ZnO Nanorods. The morphology of the ZnO NR matrix on the Pt SPEs was investigated by FESEM, as shown in Figure 3. The inset of Figure 3(a) is a picture of the sensor chip based on ZnO NR-modified Pt SPEs, which involves the Pt counter electrode, the Pt pseudoreference electrode, and the ZnO NR working electrode. Vertical ZnO NRs were successfully grown on the patterned Pt working electrode. Figure 3(b) shows a higher magnification top-view of the grown ZnO NR matrix. The as-prepared ZnO NRs have a clear hexagonal cross section with a diameter and a length of around 20-200 nm and 5-7 μm, respectively. The NRs were firmly grown and uniformly distributed over the entire circular working electrode substrate. The growth mechanism of ZnO NRs has been discussed in detail in references [35, 36].

The crystal structure of the ZnO NRs grown on Pt electrode was analyzed by XRD, and the result is shown in Figure 4.

The diffraction peaks of the ZnO NRs can be indexed to the standard profile of the wurtzite ZnO (JCPDS 36-1451)

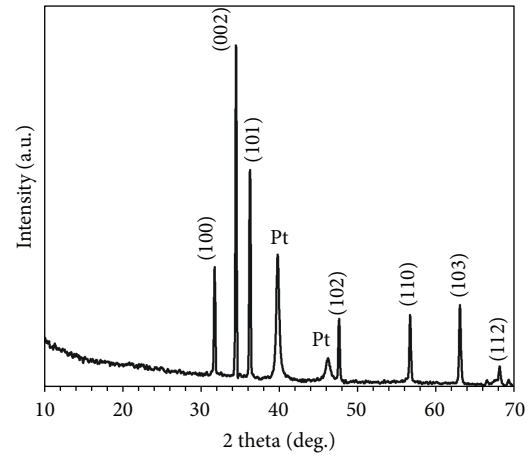

Figure 4: XRD pattern of hydrothermally grown ZnO NRs.

[13]. Two extra peaks at $2\theta = 40^\circ$ and 46.5° were indexed to the Pt layer coated over the silicon substrate. No other peaks are present, signifying the absence of any impurity or intermediate formation during growth. Sharp and intense diffraction peaks confirm a high degree of crystallization of ZnO NRs.

Morphology and crystalline structure of the ZnO NRs were confirmed by HRTEM analysis, as shown in Figure 5. Figure 5(a) illustrates a low magnification TEM image of ZnO NRs with diameters around 30 nm. The lattice fringes of about 2.38 Å are visible in Figure 5(b), confirming the good monocrystallinity of the NRs. The lattice fringes are consistent with the [0001] direction of hexagonal ZnO [12].

3.2. Electrochemical Measurements. To study the influence of the substrate modification on the performance of the sensing device, two kinds of electrodes including bare platinum SPEs and ZnO NR-modified platinum SPEs were investigated. The antibody (anti-*Salmonella* Ab) was immobilized on a self-assembled monolayer (SAM) on electrodes using the same synthesis protocol as described in Section 2.4.

Cyclic voltammetry (CV) in a solution containing 5 mM $[Fe(CN)_6]^{3-/4-}$ at 100 mV/s scan rate gives a typical sigmoid curve with steady state diffusion limited currents, as shown in

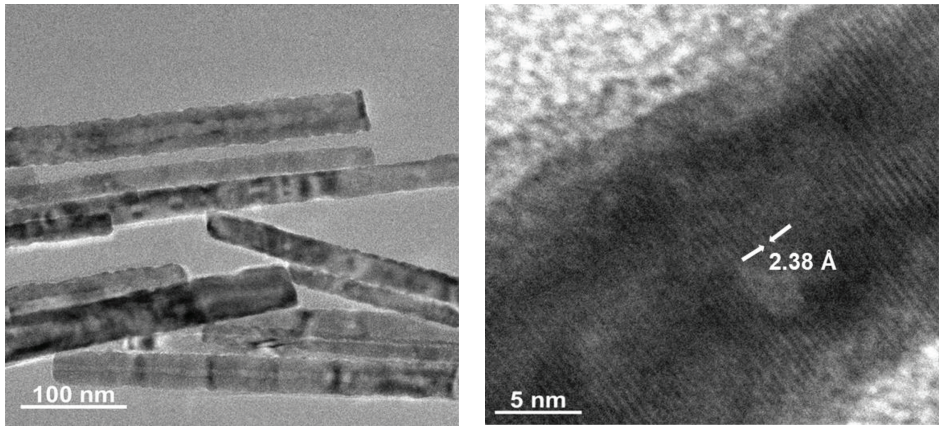

(a) (b)

Figure 5: HRTEM images of ZnO NRs at (a) low and (b) high magnification.

Figure 6. The CV plot from the ZnO NR-modified working electrode (Figure 6, the red curve) shows lower redox peaks than those from the bare Pt electrode (Figure 6, the black curve), indicating a larger resistance associated with the ZnO NR modification. After the antibody immobilization onto the surface of ZnO NR-modified Pt SPEs, the peak currents of $[Fe(CN)_6]^{3-/4-}$ decreased (Figure 6, the blue curve). This can be explained by the formation of a monolayer of antibodies on the surface of electrodes that could hinder the charge transfer to a certain extent. After incubation with the sample solution, this layer could be thicker based on the specific reaction of antigen-antibody on the electrode surface; indeed, the redox peak currents further decreased (Figure 6, the dark-cyan curve). This might be attributed to the negatively charged antibody, which obstructed the transfer of charges. The redox peak currents of antibody-immobilized ZnO NR-Pt SPEs were stable after 20 cycles of CV scanning. This confirmed the significant bond strength between ZnO NR-antibody via the crosslinkers. After the *Salmonella* bacteria was incubated on the working electrode surface for 30 min, the redox peak currents steeply decreased (Figure 6, the dark-cyan curve). This might be attributed to the thick layer of antibody-*Salmonella* bacteria binding which inhibited the electron transfer from the electrolytic solution to the electrode.

To explain more clearly the phenomenon on the surface of electrodes, electrochemical impedance spectroscopy (EIS) was investigated. Thus, the impedimetric measurements of ZnO NR-modified Pt SPEs have been performed before and after antibody immobilization and also after the incubation of bacterial antigens, as shown in Figure 7. Nyquist plots were used to investigate the change in the electron transfer resistance at the interface between working electrodes and electrolytic solution after each modification step.

The semicircle diameter at higher frequencies was related to the charge transfer resistance (R_{ct}) that controls the charge transfer kinetics of the redox probe at the electrode interface. As can be seen from Figure 7, the bare Pt SPEs exhibited a small semicircle due to the fast charge transfer process (Figure 7, the black curve, which was presented in the inset).

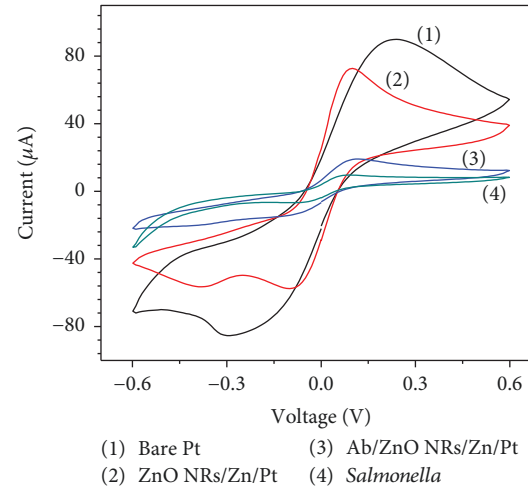

Figure 6: The CV of ZnO NR-modified Pt SPEs in response to 10^3 cfu/mL of *Salmonella* bacteria incubated for 30 min and measured in a solution containing 5 mM $[Fe(CN)_6]^{3-/4-}$ at a scan rate of 100 mV/s, with 20 cycles.

It is the EIS of the bare platinum SPEs zoomed in; the Nyquist plots did not come from the point of origin between Z' and Z'' axes (real and imaginary parts). They started from the values of around 200 ohm of the Z' axis because of the solution resistance. In fact, Pt is a metal with a high electrical conductivity. After the modification of the Pt electrode surface with ZnO NRs, the charge transfer resistance R_{ct} of the device became higher (Figure 7, the red curve), indicating that ZnO NRs could detain the charge transfer as a semiconductor material. When the antibody was immobilized on the working electrodes' surface, the resistance value significantly increased, implying that the antibody hindered the charge transfer to the electrode as an additional barrier (Figure 7, the blue curve). Subsequently, after the reaction of bacterial antigen-antibody, the layer at the electrode surface becomes thicker and the resistance steeply rose even after 5 cycles of CV scanning (Figure 7, the dark-cyan curve). The Randles

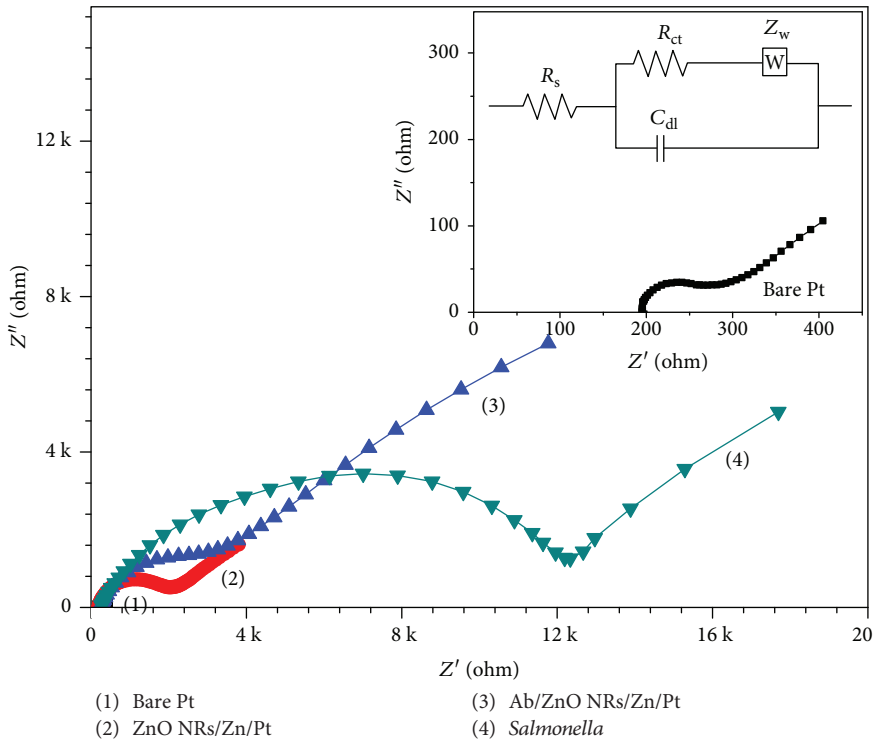

Figure 7: The Nyquist plot of ZnO NR-modified Pt electrode exposed to 10^3 cfu/mL *Salmonella*, measured in a solution containing 5 mM $[Fe(CN)_6]^{3-/4-}$. Inset: the Nyquist plot of the bare Pt SPEs; the equivalent Randles circuit: R_s: electrolytic solution resistance, R_{ct}: charge transfer resistance, and Z_w: Warburg impedance.

equivalent circuit of the modified SPEs is also provided in Figure 7.

For ZnO NR-modified Pt SPEs, factors such as high antibody binding and electron transfer rate play a major role. In this work, all the experiments were performed at pH of 7.4 to retain its bioactivity but also accelerate charge transfer communication between antigen and the electrode to a large extent [9].

The respective semicircle diameter corresponds to the charge transfer resistance (R_{ct}), the values of which are calculated using the fitting program IviumSoft (developed by Ivium Technologies, Netherlands) (Table 1). After antibody immobilization of the ZnO NR-modified Pt SPE surface, the mean R_{ct} value was calculated as about 2,536 Ω after 5 cycles of CV scanning, which is 1.56-fold higher than the 1,621 Ω obtained with the ZnO NR-modified Pt SPEs. This indicates a clear verification that antibodies have been successfully immobilized onto the platinum surface and remained during the electrochemical process. The higher R_{ct} value can best be explained by reduced efficiency of the redox couple, $[Fe(CN)_6]^{3-/4-}$, to reach the electrode surface in the presence of antibody, presumably due to charge repulsion between the negatively charged antibody and $[Fe(CN)_6]^{3-/4-}$ [37]. After the *Salmonella* bacteria interacted on the electrode surface, the mean R_{ct} quickly increased, reaching 9,158 Ω after 5 cycles of CV scanning. This might be attributed to the thicker layer of bacteria-antibody formed, which obstructed the transfer of charges, as discussed above. These results were consistent with the results obtained from CV. After the same scan cycles of CV, the mean R_{ct} values of ZnO NR-modified Pt SPEs after antibody immobilization and *E. coli* incubation were much lower, 2,791 Ω and 3,016 Ω, respectively. It is reasonable to suppose that most unspecific elements have been removed from the electrodes during washing steps and CV scanning as well. However, there are still some elements bounded on the electrodes due to the space obstruction. It also confirms that ZnO NR-modified Pt SPEs were successfully used for the detection of *Salmonella* bacteria at the concentration of 10^3 cfu/mL and could be optimized for the further development of biochips for electrochemical detection of other pathogens.

Table 1: The R_{ct} values varied according to the changes on the surface of modified SPEs.

Sample	R_{ct} (ohm)
Pt SPEs	76.66 ± 0.42
ZnO NR-modified Pt SPEs	1,621.00 ± 81.05
Ab/ZnO NR-modified Pt SPEs	2,536.00 ± 177.52
Salmonella-Ab/ZnO NR-modified Pt SPEs	9,158.00 ± 457.90
BSA-Ab/ZnO NR-modified Pt SPEs	2,791.00 ± 167.46
E. coli-Ab/ZnO NR-modified Pt SPEs	3,016.00 ± 211.12

4. Conclusions

This study revealed that potential biosensors which could be developed from Pt SPEs modified with vertical ZnO NRs on

the working electrode for electrochemical detection of bacterial pathogens. The morphological and structural investigation showed that the ZnO NR matrix was well-patterned and firmly grown on the Pt working electrode without impurities. CV and EIS measurements proved the stability in the detection of *Salmonella* bacteria at the concentration of 10^3 cfu/mL. The study opens opportunities for further development of electrochemical biochips based on ZnO NR-modified Pt SPEs for the expansion of rapid and accurate detection systems for highly pathogenic bacteria.

Data Availability

The data used to support the findings of this study are available from the corresponding authors upon request.

Conflicts of Interest

The authors declare that there is no conflict of interests regarding the publication of this paper.

Acknowledgments

This research is funded by Vietnam National Foundation for Science and Technology Development (NAFOSTED) under grant number 103.02-2015.43.

References

[1] P. B. Luppa, L. J. Sokoll, and D. W. Chan, "Immunosensors—principles and applications to clinical chemistry," *Clinica Chimica Acta*, vol. 314, no. 1-2, pp. 1–26, 2001.

[2] E. Katz and I. Willner, "Probing biomolecular interactions at conductive and semiconductive surfaces by impedance spectroscopy: routes to impedimetric immunosensors, DNA-sensors, and enzyme biosensors," *Electroanalysis*, vol. 15, no. 11, pp. 913–947, 2003.

[3] M. Pumera, S. Sánchez, I. Ichinose, and J. Tang, "Electrochemical nanobiosensors," *Sensors and Actuators B: Chemical*, vol. 123, no. 2, pp. 1195–1205, 2007.

[4] A. Tereshchenko, M. Bechelany, R. Viter et al., "Optical biosensors based on ZnO nanostructures: advantages and perspectives. A review," *Sensors and Actuators B: Chemical*, vol. 229, pp. 664–677, 2016.

[5] M. Dequaire and A. Heller, "Screen printing of nucleic acid detecting carbon electrodes," *Analytical Chemistry*, vol. 74, no. 17, pp. 4370–4377, 2002.

[6] Y.-H. Lin, S.-H. Chen, Y.-C. Chuang et al., "Disposable amperometric immunosensing strips fabricated by Au nanoparticles-modified screen-printed carbon electrodes for the detection of foodborne pathogen Escherichia coli O157:H7," *Biosensors & Bioelectronics*, vol. 23, no. 12, pp. 1832–1837, 2008.

[7] L. Falciola, V. Pifferi, and E. Mascheroni, "Platinum-based and carbon-based screen printed electrodes for the determination of benzidine by differential pulse voltammetry," *Electroanalysis*, vol. 24, no. 4, pp. 767–775, 2012.

[8] S. K. Arya, S. Saha, J. E. Ramirez-Vick, V. Gupta, S. Bhansali, and S. P. Singh, "Recent advances in ZnO nanostructures and thin films for biosensor applications: review," *Analytica Chimica Acta*, vol. 737, pp. 1–21, 2012.

[9] A. A. Ansari, A. Kaushik, P. R. Solanki, and B. D. Malhotra, "Nanostructured zinc oxide platform for mycotoxin detection," *Bioelectrochemistry*, vol. 77, no. 2, pp. 75–81, 2010.

[10] P. R. Solanki, A. Kaushik, V. V. Agrawal, and B. D. Malhotra, "Nanostructured metal oxide-based biosensors," *NPG Asia Materials*, vol. 3, no. 1, pp. 17–24, 2011.

[11] P. Pashazadeh, A. Mokhtarzadeh, M. Hasanzadeh, M. Hejazi, M. Hashemi, and M. de la Guardia, "Nano-materials for use in sensing of salmonella infections: recent advances," *Biosensors & Bioelectronics*, vol. 87, pp. 1050–1064, 2017.

[12] M. Tonezzer, T. T. L. Dang, N. Bazzanella, V. H. Nguyen, and S. Iannotta, "Comparative gas-sensing performance of 1D and 2D ZnO nanostructures," *Sensors and Actuators B: Chemical*, vol. 220, pp. 1152–1160, 2015.

[13] L. Vayssieres, "Growth of arrayed nanorods and nanowires of ZnO from aqueous solutions," *Advanced Materials*, vol. 15, no. 5, pp. 464–466, 2003.

[14] N. Phu Huong Lan, T. Le Thi Phuong, H. Nguyen Huu et al., "Invasive non-typhoidal Salmonella infections in Asia: clinical observations, disease outcome and dominant serovars from an infectious disease hospital in Vietnam," *PLoS Neglected Tropical Diseases*, vol. 10, no. 8, article e0004857, 2016.

[15] M. Jiao, N. V. Chien, N. V. Duy et al., "On-chip hydrothermal growth of ZnO nanorods at low temperature for highly selective NO_2 gas sensor," *Materials Letters*, vol. 169, pp. 231–235, 2016.

[16] Z. Yang, M. Wang, Q. Zhao et al., "Dielectrophoretic-assembled single and parallel-aligned Ag nanowire–ZnO-branched nanorod heteronanowire ultraviolet photodetectors," *ACS Applied Materials & Interfaces*, vol. 9, no. 27, pp. 22837–22845, 2017.

[17] O. Lupan, L. Chow, G. Chai, L. Chernyak, O. Lopatiuk-Tirpak, and H. Heinrich, "Focused-ion-beam fabrication of ZnO nanorod-based UV photodetector using the in-situ lift-out technique," *Physica Status Solidi*, vol. 205, no. 11, pp. 2673–2678, 2008.

[18] T. Van Dang, N. Duc Hoa, N. Van Duy, and N. Van Hieu, "Chlorine gas sensing performance of on-chip grown ZnO, WO_3, and SnO_2 nanowire sensors," *ACS Applied Materials & Interfaces*, vol. 8, no. 7, pp. 4828–4837, 2016.

[19] L. Q. Toan, H. Nguyen-Viet, and B. M. Huong, "Risk assessment of Salmonella in pork in Hanoi, Vietnam," *Vietnamese Journal of Preventive Medicine*, vol. 23, no. 4, pp. 10–17, 2013.

[20] L. Q. Huong, F. Reinhard, P. Padungtod et al., "Prevalence of *Salmonella* in retail chicken meat in Hanoi, Vietnam," *Annals of the New York Academy of Sciences*, vol. 1081, no. 1, pp. 257–261, 2006.

[21] T. T. Le Dang, M. Tonezzer, and V. H. Nguyen, "Hydrothermal growth and hydrogen selective sensing of nickel oxide nanowires," *Journal of Nanomaterials*, vol. 2015, Article ID 785856, 8 pages, 2015.

[22] G. Fiaschi, S. Cosentino, R. Pandey et al., "A novel gas-phase mono and bimetallic clusters decorated ZnO nanorods electrochemical sensor for 4-aminophenol detection," *Journal of Electroanalytical Chemistry*, vol. 811, pp. 89–95, 2018.

[23] D. T. A. Nguyen, M. Kanki, P. D. Nguyen et al., "Prevalence, antibiotic resistance, and extended-spectrum and AmpC β-lactamase productivity of Salmonella isolates from raw meat and seafood samples in Ho Chi Minh City, Vietnam," *International Journal of Food Microbiology*, vol. 236, pp. 115–122, 2016.

[24] S. Park, B. Szonyi, R. Gautam, K. Nightingale, J. Anciso, and R. Ivanek, "Risk factors for microbial contamination in fruits and vegetables at the preharvest level: a systematic review," *Journal of Food Protection*, vol. 75, no. 11, pp. 2055–2081, 2012.

[25] J. Guard-Petter, "The chicken, the egg and Salmonella enteritidis," *Environmental Microbiology*, vol. 3, no. 7, pp. 421–430, 2001.

[26] V. Nandakumar, J. T. La Belle, J. Reed et al., "A methodology for rapid detection of Salmonella typhimurium using label-free electrochemical impedance spectroscopy," *Biosensors & Bioelectronics*, vol. 24, no. 4, pp. 1039–1042, 2008.

[27] S. Cinti, G. Volpe, S. Piermarini, E. Delibato, and G. Palleschi, "Electrochemical biosensors for rapid detection of foodborne Salmonella: a critical overview," *Sensors*, vol. 17, no. 8, p. 1910, 2017.

[28] D. T. T. Le, N. V. Hoang, N. V. Hieu, V. Q. Khue, and T. Q. Huy, "Fabrication of electrochemical electrodes based on platinum and ZnO nanofibers for biosensing applications," *Communications on Physics*, vol. 27, no. 3, pp. 221–231, 2017.

[29] M. Jiao, N. Van Duy, D. D. Trung et al., "Comparison of NO_2 gas-sensing properties of three different ZnO nanostructures synthesized by on-chip low-temperature hydrothermal growth," *Journal of Electronic Materials*, vol. 47, no. 1, pp. 785–793, 2018.

[30] V. T. Duoc, D. T. T. Le, N. D. Hoa et al., "New design of ZnO nanorod- and nanowire-based NO_2 room-temperature sensors prepared by hydrothermal method," *Journal of Nanomaterials*, vol. 2019, Article ID 6821937, 9 pages, 2019.

[31] R. M. Petoral Jr., G. R. Yazdi, A. Lloyd Spetz, R. Yakimova, and K. Uvdal, "Organosilane-functionalized wide band gap semiconductor surfaces," *Applied Physics Letters*, vol. 90, no. 22, article 223904, 2007.

[32] C. D. Corso, A. Dickherber, and W. D. Hunt, "An investigation of antibody immobilization methods employing organosilanes on planar ZnO surfaces for biosensor applications," *Biosensors & Bioelectronics*, vol. 24, no. 4, pp. 805–811, 2008.

[33] S. K. Bhatia, L. C. Shriver-Lake, K. J. Prior et al., "Use of thiol-terminal silanes and heterobifunctional crosslinkers for immobilization of antibodies on silica surfaces," *Analytical Biochemistry*, vol. 178, no. 2, pp. 408–413, 1989.

[34] P. Sanguino, T. Monteiro, S. R. Bhattacharyya, C. J. Dias, R. Igreja, and R. Franco, "ZnO nanorods as immobilization layers for interdigitated capacitive immunosensors," *Sensors and Actuators B: Chemical*, vol. 204, pp. 211–217, 2014.

[35] S. Baruah and J. Dutta, "Hydrothermal growth of ZnO nanostructures," *Science and Technology of Advanced Materials*, vol. 10, no. 1, article 13001, 2016.

[36] T. R. Chetia, M. S. Ansari, and M. Qureshi, "Graphitic carbon nitride as a photovoltaic booster in quantum dot sensitized solar cells: a synergistic approach for enhanced charge separation and injection," *Journal of Materials Chemistry A*, vol. 4, no. 15, pp. 5528–5541, 2016.

[37] F. Rohrbach, H. Karadeniz, A. Erdem, M. Famulok, and G. Mayer, "Label-free impedimetric aptasensor for lysozyme detection based on carbon nanotube-modified screen-printed electrodes," *Analytical Biochemistry*, vol. 421, no. 2, pp. 454–459, 2012.